

Published in final edited form as:

Magn Reson Med. 2014 August ; 72(2): 464–470. doi:10.1002/mrm.24951.

On the Confounding Effect of Temperature on Chemical Shift-Encoded Fat Quantification

Diego Hernando^{1,*}, Samir D. Sharma¹, Harald Kramer^{1,2}, and Scott B. Reeder^{1,3,4,5}

¹Department of Radiology, University of Wisconsin, Madison, Wisconsin, USA

²Institute for Clinical Radiology, Ludwig-Maximilians-University Hospital Munich, Munich, Germany

³Department of Medicine, University of Wisconsin, Madison, Wisconsin, USA

⁴Department of Medical Physics, University of Wisconsin, Madison, Wisconsin, USA

⁵Department of Biomedical Engineering, University of Wisconsin, Madison, Wisconsin, USA

Abstract

Purpose—To characterize the confounding effect of temperature on chemical shift-encoded (CSE) fat quantification.

Methods—The proton resonance frequency of water, unlike triglycerides, depends on temperature. This leads to a temperature dependence of the spectral models of fat (relative to water) that are commonly used by CSE-MRI methods. Simulation analysis was performed for 1.5 Tesla CSE fat–water signals at various temperatures and echo time combinations. Oil–water phantoms were constructed and scanned at temperatures between 0 and 40°C using spectroscopy and CSE imaging at three echo time combinations. An explanted human liver, rejected for transplantation due to steatosis, was scanned using spectroscopy and CSE imaging. Fat–water reconstructions were performed using four different techniques: magnitude and complex fitting, with standard or temperature-corrected signal modeling.

Results—In all experiments, magnitude fitting with standard signal modeling resulted in large fat quantification errors. Errors were largest for echo time combinations near $TE_{\text{init}} \approx 1.3$ ms, $TE \approx 2.2$ ms. Errors in fat quantification caused by temperature-related frequency shifts were smaller with complex fitting, and were avoided using a temperature-corrected signal model.

Conclusion—Temperature is a confounding factor for fat quantification. If not accounted for, it can result in large errors in fat quantifications in phantom and ex vivo acquisitions.

Keywords

temperature; fat quantification; proton-density fat-fraction; confounding factors; liver imaging; fat; water imaging

INTRODUCTION

In recent years, tremendous progress has been made on the development and validation of confounder-corrected chemical shift-encoded fat–water imaging methods for accurate quantitation of fat content (1–10). When all confounders are successfully addressed, these methods provide accurate estimates of the proton density fat-fraction (PDFF) (11). Emerging methods that have demonstrated accuracy and robustness perform correction for multiple confounding factors, which include T1-related bias (12), R2* decay (13–18), noise-related bias (12), and the spectral complexity of fat (8,14). Magnitude methods, which retain only the magnitude of the acquired images (13,19), complex methods that use both the phase and the magnitude information (16,17), as well as hybrid/mixed methods (20,21), have been described.

Considerable work has been performed to demonstrate the importance of accurate spectral modeling of fat to ensure accurate measurements of fat content (8–10,22). Spectral modeling of fat accounts for the proton signals from the various resonance peaks of triglycerides. When accounted for, more accurate estimates of PDFF are achieved, and the estimate of PDFF is robust to changes in echo time (TE) choices and the number of echoes (23). Additionally, recent reports demonstrate the importance of using the correct spectral model when performing fat-corrected R2* estimation in the liver (18,24,25).

It is well known that the proton resonance frequency (PRF) of water is dependent on temperature (26–32). Importantly, the PRF of fat does not change with temperature (aside from volume susceptibility variations), and therefore the relative chemical shift between the water resonance and the multiple fat resonances will depend on temperature (30,31,33). This effect has been exploited to measure the temperature within tissues that contain both water and fat using chemical shift-encoded imaging methods (34–36).

Given the importance of accurate spectral modeling of fat, which includes the relative chemical shift between the water peak and fat peaks, the effects of temperature may be important for accurate fat quantification in tissues or materials at varying temperature. This is particularly relevant for phantom experiments, animal experiments performed under anesthesia, and measurement of fat content in tissue specimens that are not at body temperature.

Therefore, the purpose of this work was to investigate the effects of temperature as a confounding factor of fat quantification using chemical shift-encoded methods, through the effect of temperature on the PRF of water. Specifically, the effects of temperature on fat quantification will be investigated, including the impact of echotime choice and choice of reconstruction method.

THEORY

In MR acquisitions, the proton resonance frequency (PRF) has a well-documented dependence on temperature (26,27,35,37). This effect is caused by the temperature dependence of: (i) electronic shielding of protons, and (ii) volume susceptibility (27,38). The PRF of water is dependent on both electronic shielding and volume susceptibility, whereas

the PRF of fat is only dependent on volume susceptibility (32,38). Thus, in mixtures of water and fat, temperature changes will result in a bulk frequency offset due to susceptibility variations, and additionally a change in the fat–water frequency shift due to changes in the electronic shielding of water protons (38).

Accounting for temperature effects, the spoiled gradient-echo (SPGR) signal from a voxel containing both fat and water can be modeled as (16,26,27,35):

$$S_T(T E_n) = (W e^{i2\pi f_T T E_n} + F c_n) e^{i2\pi f_B T E_n} e^{-R_2^* T E_n} \quad [1]$$

where W and F are the (complex-valued) amplitudes of water and fat signals, respectively, $c_n = \sum_{p=1}^P \alpha_p e^{i2\pi f_{F,p} T E_n}$ is the multi-peak fat signal model consisting of P peaks with amplitudes α_p and frequencies $f_{F,p}$, as described in previous works (16,39), f_B is the bulk frequency shift due to local magnetic B_0 field inhomogeneities (including temperature-dependent volume susceptibility effects) (32), $R_2^* = 1/T_2^*$, and f_T (in Hz) is the frequency offset of water due to temperature effects on the electronic shielding of water protons. The parameter f_T has a dependence on temperature of nearly $-0.01 \text{ ppm}/^\circ\text{C} \approx -0.64 \text{ Hz}/^\circ\text{C}$ at 1.5 Tesla (T) (26,27,35). For instance, a temperature change of 10°C will result in a change of nearly -6.4 Hz in the fat–water frequency shift at 1.5T. Because the water signal is typically considered to be on resonance, the signal model in Eq. [1] can be rewritten as:

$$\begin{aligned} S_T(T E_n) &= (W + F c_n e^{-i2\pi f_T T E_n}) e^{i2\pi (f_B + f_T) T E_n} e^{-R_2^* T E_n} \quad [2] \\ &= (W + F c_{T,n}) e^{i2\pi f'_B T E_n} e^{-R_2^* T E_n} \quad [3] \end{aligned}$$

where the variation in the fat–water frequency shift is incorporated into the multi-peak fat signal model, i.e.: $c_{T,n} = c_n e^{-i2\pi f_T T E_n}$, and the observed *effective* B_0 offset includes the corresponding temperature dependent shift, i.e.: $f'_B = f_B + f_T$.

Fat quantification from SPGR acquisitions is typically performed using the signal model in Eq. [1], assuming that $f_T = 0$, to fit the acquired signal. This can be accomplished through complex-based and magnitude-based methods (14). Complex-based methods use the phase and magnitude of the acquired signal (16). Magnitude-based methods discard the signal phase, and are often used in quantitative applications to avoid phase errors (e.g., due to eddy currents) (13,20).

The effective observed B_0 offset has no impact on fat quantification, because it simply introduces a bulk frequency shift on the acquired signal, which is estimated in complex methods and discarded in magnitude methods. However, the modified fat signal model $c_{T,n}$ results in a temperature-dependent model mismatch if not accounted for. This model mismatch may result in systematic errors in fat quantification, and in principle these errors may be dependent on acquisition parameters (e.g., TEs), and reconstruction technique (e.g., complex or magnitude). In this work, we characterize the effects of temperature on fat quantification accuracy using simulations, phantom experiments, and ex vivo liver experiments.

METHODS

Simulations

Simulated multi-echo fat–water signals were synthesized at 1.5T using Eq. [3] with $f'_B = 0$ Hz, $R2^* = 40\text{s}^{-1}$ for fat-fractions between 0 and 50%. Noiseless signals were generated for different six-echo combinations, using initial TE values between 0 and 3.3 ms, and TE spacing between 0.4 and 3 ms. Signals were generated using a spectral model of fat from the liver (39), with different temperature-related fat–water frequency shifts between 3.8 ppm and 3.35 ppm (frequency shift between water and the main methylene fat, corresponding to temperatures approximately between 0°C and 40°C).

For each multi-echo signal, four fat–water reconstructions were performed by fitting the signal model in Eq. [3] to the synthesized data, using: magnitude or complex fitting, in combination with the “standard” (temperature-uncorrected) *in vivo* signal model with fat–water frequency shift 3.4 ppm (corresponding to a body temperature of 37°C) or the “temperature-corrected” signal model with the same frequency shift used to generate the data. From each of these reconstructions, fat-fraction was calculated as $FF = 100 \times F/(W + F)$.

Phantom Experiments

Phantom Construction and Setup—A fat–water phantom was constructed according to the method of Hines et al (40), without iron, and using a higher concentration of CuSO_4 (3 mM) to minimize T1 bias. The phantom was comprised of eight cylindrical vials (approximate diameter = 22 mm, height = 53 mm) with oil–water emulsions including nominal FFs of 0, 5, 10, 20, 30, 40, 50, and 100%, respectively. After adjusting for lost water volume (40), expected fat-fractions were 0, 5.3, 10.5, 20.9, 31.2, 41.3, 51.4, and 100%, respectively.

The vials were fixed inside a plastic container, and an MR-compatible fiber optic temperature sensor (REFLEX-4, Neoptix, Quebec, Canada) was inserted next to the vials. The temperature probe was connected to a monitoring system, set to record the temperature automatically every 60 s. The plastic container was filled with ice water, and placed in a 1.5T clinical MRI scanner (Signa HDxt, GE Healthcare, Waukesha, WI), where it was scanned at temperature intervals of approximately 2°C, as the water warmed to room temperature. This required approximately 5 hours. Because of the slow temperature variation, the phantom vials were assumed to be at the same temperature as the surrounding water. Next, the same setup was used, except that the plastic container was initially filled with warm water (40°C), and data were acquired as the water cooled down to room temperature. Because the change in temperature was very slow as it approached room temperature, two additional acquisitions were performed by directly filling up the container with water at temperatures 18°C and 22°C.

MR Spectroscopy—For each temperature, a single-voxel MRS spectrum was obtained from the FF = 50% vial using a stimulated echo acquisition mode (STEAM) sequence with TE = 10 ms, repetition time (TR) = 3500 ms, 2048 readout points, 1 average, and spectral

width = ± 2.5 kHz. Spectroscopy data were used to estimate the fat–water frequency shift at each temperature. An offline custom Matlab (Mathworks, Natick, MA) routine was used to determine f_T using Eq. [2] to fit the spectroscopy data. Note that scanner B_0 drift effects over the course of the experiment will not introduce errors in this technique, because they will not significantly affect the frequency shift between fat and water.

MR Imaging—Chemical shift-encoded data were acquired using an investigational version of a three-dimensional multi-echo SPGR sequence with monopolar readouts and flyback gradients (8). To test the effects of TE combination on temperature-related bias, three different acquisitions were performed, with different 6-echo TE combinations: (a) Protocol 1: $TE_{init} = 1.04$ ms, $TE = 1.69$ ms; (b) Protocol 2: $TE_{init} = 1.24$ ms, $TE = 2.06$ ms; (c) Protocol 3: $TE_{init} = 1.34$ ms, $TE = 2.25$ ms.

These TE combinations were chosen based on preliminary simulations (not shown), because they were expected to result in different temperature-related fat quantification errors. Other acquisition parameters included: axial plane, readout direction R/L, field-of-view 40×28 cm², 192–256 readout samples, 160 phase encoding steps, 4 mm slice thickness, 24 slices, 5° flip angle, ± 94 –125 kHz receiver bandwidth (adjusted to change TE), TR=12.0–15.3 ms. These three chemical shift-encoded acquisitions were repeatedly performed over the range of temperatures 0–40°C.

MR imaging data were reconstructed using four different fat-fraction reconstruction algorithms, as in the simulation data. The model for multi-peak fat spectrum in phantoms (peanut oil) was derived based on Bydder et al (41), using the routine provided within the ISMRM Fat–Water Toolbox (42). The temperature-corrected model c_T was determined in each case using the fat–water frequency shift measured from the spectroscopy data.

Ex Vivo Experiments

An explanted cadaveric human liver, intended for orthotopic liver transplantation but rejected due to hepatic steatosis per standard protocol (43) was studied. Originally packaged in ice, the explanted liver was removed from the ice approximately 20 min before imaging. The temperature of the liver was not measured.

The liver was placed in a plastic bag and subsequently placed in a bath of water at room temperature. Data were acquired in the same 1.5T scanner used for the phantom experiments. Four STEAM-MRS spectra were obtained throughout the liver (at locations corresponding approximately to Couinaud segments 3–6), and used as a reference for fat quantification (39,44). STEAM spectra were acquired from volumes of approximate dimensions $20 \times 20 \times 20$ mm³, with five TEs between 10 ms and 30 ms to enable T2 correction. Other acquisition parameters for STEAM included: TR=3500 ms, 2048 readout points, 1 average, and spectral width = ± 2.5 kHz. Spectroscopic quantification of fat was performed using the AMARES algorithm (39,45) within the jMRUI package (46). Each of the four STEAM spectra was processed and the resulting FFs were averaged to obtain a liver spectroscopy-based reference FF measurement.

Chemical shift-encoded imaging (multi-echo SPGR) was performed using the following acquisition parameters: axial plane, readout direction R/L, 44×44 cm field of view, 256×160 matrix, 8 mm slice thickness, 32 slices, 5° flip angle, ± 125 kHz receiver bandwidth, TR=13.6 ms, and 6 echoes ($TE_{\text{init}} = 1.20$ ms, $TE = 1.98$ ms). Imaging data were reconstructed using the same four reconstructions as in simulation and phantom data, with a multi-peak model of fat derived for liver fat (39). For the temperature-corrected reconstructions, the fat–water shift was assessed from spectroscopy data. From each of the four imaging reconstructions, imaging FF was assessed using measurements colocalized with the spectroscopy volumes, and these measurements were averaged to obtain an imaging-based liver FF measurement.

RESULTS

Figure 1 shows simulation results for fat quantification bias in the presence of temperature-related model mismatch. As observed in this figure, complex fitting results in fat quantification errors, but these errors are moderate over all echo combinations tested. Magnitude fitting results in errors slightly higher than those of complex fitting over a wide range of echo combinations, but results in severe bias (e.g., $>20\%$ absolute error in FF) for certain echo combinations, particularly those near ($TE_{\text{init}} = 1.3$ ms, $TE=2.2$ ms). The reason for the large errors occurring at these particular echo combinations with magnitude fitting is that water and the main methylene peak of fat are in quadrature, i.e., $s(TE_n) \approx W + iF(-1)^n$. With this combination of echoes, all information about the relative amount of water and fat is lost because the signal magnitude $|s(TE_n)| \approx \sqrt{W^2 + F^2}$ becomes nearly invariant with TE. For these echo combinations, the magnitude signal contains little information that would enable fat–water separation, and is very sensitive to noise (21,47) or model mismatch.

Figure 2 shows the dependence of fat–water frequency shift as a function of temperature, measured from spectroscopy in the vial with FF = 50%. A linear dependence was observed with strong correlation ($r^2 = 0.997$). The measured slope (-0.01085 ± 0.00015 ppm/ $^\circ\text{C}$) was in good agreement with literature values (nearly -0.01 ppm/ $^\circ\text{C}$, with slight variability depending on the specific sample being scanned) (26,27,35,37).

Figure 3 shows phantom fat quantification results over temperatures between 0°C and 40°C for magnitude/complex and standard/temperature-corrected reconstructions. In Figure 3a, the temperature dependence of FF errors is shown explicitly for a vial with FF = 31.2%. Simulation results are also shown for comparison. For protocol 1, moderate FF errors ($<5\%$) are encountered with all reconstructions over a wide range of temperatures (15°C – 40°C). For protocols 2–3, the standard reconstructions result in severe errors, particularly for magnitude reconstructions. These errors are largely mitigated when a temperature-corrected model of fat is used.

The absolute FF errors for temperature-corrected complex fitting were all less than 4.7% over all vials, protocols, and temperatures. Temperature correction also resulted in good accuracy for magnitude fitting, with the exception of protocol 2 at low temperatures, where temperature-corrected magnitude reconstructions were extremely noisy. This poor noise

performance is well explained by the higher fat–water frequency shift used in the temperature-corrected reconstruction, which results in poor SNR performance of magnitude fitting for the specific echo combination in protocol 2 (see Figure 4).

Figure 5 shows the explanted liver reconstructions, and a representative STEAM spectrum including both water and fat peaks, with measured frequency shift 3.67 ppm. Standard magnitude fitting resulted in large negative bias (similarly to the simulations), whereas complex fitting or temperature-corrected magnitude fitting resulted in improved agreement with the spectroscopy reference (FF = 9.3%). Furthermore, there is an apparent spatial heterogeneity in fat-fraction maps, particularly in the standard magnitude reconstruction. The source of this apparent heterogeneity is unclear, but we speculate that it is due to temperature heterogeneity within the explanted liver (which is likely warmer near the edges compared with the center), due to insufficient time for full warming to room temperature.

DISCUSSION

In this work, we have demonstrated that temperature is a confounding factor for the quantification of fat using chemical shift-encoded fat–water imaging techniques. By altering the fat–water frequency shift through changes in the water PRF, the spectral model between water and fat is altered. This leads to errors in fat quantification that are highly dependent on the choice of TEs, as well as the reconstruction method used to estimate PDF. Magnitude-based reconstruction methods (or hybrid methods that largely rely on a magnitude-based estimate) are more sensitive to temperature effects than complex-based methods.

It is important to consider the effects of temperature on the spectral model of fat for several reasons. Emerging chemical shift-encoded methods that are commercially available have spectral models of fat that are based on *in vivo* temperature, i.e., body temperature, and application of these methods to other systems not at this temperature could lead to potential errors in the estimate of fat-fraction. This is also important for animal studies where the animal body temperature may be different than the human body temperature, particularly under the influence of anesthesia. Another potential area of application is *ex vivo* tissue specimen testing and phantom scanning (e.g., for quality assurance of fat quantification techniques at a particular site).

Knowledge of the temperature of the sample being imaged will allow for appropriate adjustment of the fat–water frequency shift and is effective at mitigating this potential confounder. However, the SNR performance of magnitude reconstructions is sensitive to the choice of TE combination and to the PRF of water. This dependence should be taken into account when designing a protocol for scanning samples at a known temperature.

Unfortunately, it may not be possible to correct for local temperature in the image reconstruction, if the temperature varies throughout the sample being imaged. For this reason, it is important to use techniques (i.e., choice of echo combination and reconstruction method) that are robust to changes in temperature. An alternative approach would be to include the temperature-related frequency shift f_T as a free parameter in the reconstruction signal model, although this may severely affect SNR performance (36).

It is interesting to speculate whether the effects of spectral modeling are important for accurate $R2^*$ quantification using fat-corrected chemical shift-encoded methods. It has been recently demonstrated that accurate spectral modeling of fat is necessary when performing fat-corrected $R2^*$ measurements. Further work is necessary to understand the impact of temperature effects on $R2^*$ measurements.

Limitations of this study include experiments performed at only 1.5T. However, the chemical shift between water and fat is twice that at 3T, and, therefore, the general results of this work are expected to translate to 3T. Also, the explanted liver experiments did not include independent temperature measurements (aside from the indirect measurement obtained by assessing the fat–water frequency shift from spectroscopy data).

In summary, we have demonstrated that temperature effects present an important confounding factor of chemical shift-encoded fat quantification. For a given temperature, the amount of bias depends heavily on the choice of acquisition and reconstruction technique. These results may have significant implications for phantom, ex vivo tissue specimens and for in vivo animal fat quantification.

Acknowledgments

We thank Orhan Unal for assistance with the temperature probe for phantom experiments. We acknowledge the use of the ISMRM Fat-Water Toolbox (<http://ismrm.org/workshops/FatWater12/data.htm>) for some of the results shown on this article.

Grant sponsor: NIH; Grant numbers: R01 DK083380, R01 DK088925; Grant sponsor: the Wisconsin Alumni Research Foundation (WARF) Accelerator Program; Grant sponsor: the Institute for Clinical and Translational Research (ICTR); Grant sponsor: GE Healthcare.

REFERENCES

1. Bernard CP, Liney GP, Manton DJ, Turnbull LW, Langton CM. Comparison of fat quantification methods: a phantom study at 3.0T. *J Magn Reson Imaging*. 2008; 27:192–197. [PubMed: 18064714]
2. Eggers, H.; Perkins, TG.; Hussain, SM. Influence of spectral model and signal decay on hepatic fat fraction measurements at 3T with dual-echo Dixon imaging. *Proceedings of the 19th Annual Meeting of ISMRM; Montreal, Canada*. 2011. p. 573
3. Guiu B, Petit JM, Loffroy R, Ben Salem D, Aho S, Masson D, Hillon P, Krause D, Cercueil JP. Quantification of liver fat content: comparison of triple-echo chemical shift gradient-echo imaging and in vivo proton MR spectroscopy. *Radiology*. 2009; 250:95–102. [PubMed: 19092092]
4. Hussain HK, Chenevert TL, Londy FJ, Gulani V, Swanson SD, McKenna BJ, Appelman HD, Adusumilli S, Greenson JK, Conjeevaram HS. Hepatic fat fraction: MR imaging for quantitative measurement and display—early experience. *Radiology*. 2005; 237:1048–1055. [PubMed: 16237138]
5. O'Regan DP, Callaghan MF, Wylezinska-Arridge M, Fitzpatrick J, Naoumova RP, Hajnal JV, Schmitz SA. Liver fat content and $T2^*$: simultaneous measurement by using breath-hold multiecho MR imaging at 3.0 T—feasibility. *Radiology*. 2008; 247:550–557. [PubMed: 18349314]
6. Reeder SB, Sirlin CB. Quantification of liver fat with magnetic resonance imaging. *Magn Reson Imaging Clin N Am*. 2010; 18:337–357. ix. [PubMed: 21094444]
7. Hines CD, Frydrychowicz A, Hamilton G, Tudorascu DL, Vigen KK, Yu H, McKenzie CA, Sirlin CB, Brittain JH, Reeder SB. T(1) independent, T(2) (*) corrected chemical shift based fat-water separation with multi-peak fat spectral modeling is an accurate and precise measure of hepatic steatosis. *J Magn Reson Imaging*. 2011; 33:873–881. [PubMed: 21448952]

8. Meisamy S, Hines CD, Hamilton G, Sirlin CB, McKenzie CA, Yu H, Brittain JH, Reeder SB. Quantification of hepatic steatosis with T1-independent, T2-corrected MR imaging with spectral modeling of fat: blinded comparison with MR spectroscopy. *Radiology*. 2011; 258:767–775. [PubMed: 21248233]
9. Yokoo T, Bydder M, Hamilton G, et al. Nonalcoholic fatty liver disease: diagnostic and fat-grading accuracy of low-flip-angle multiecho gradient-recalled-echo MR imaging at 1.5 T. *Radiology*. 2009; 251:67–76. [PubMed: 19221054]
10. Yokoo T, Shiehorteza M, Hamilton G, et al. Estimation of hepatic proton-density fat fraction by using MR imaging at 3.0 T. *Radiology*. 2011; 258:749–759. [PubMed: 21212366]
11. Reeder SB, Hu HH, Sirlin CB. Proton density fat-fraction: a standardized MR-based biomarker of tissue fat concentration. *J Magn Reson Imaging*. 2012; 36:1011–1014. [PubMed: 22777847]
12. Liu CY, McKenzie CA, Yu H, Brittain JH, Reeder SB. Fat quantification with IDEAL gradient echo imaging: correction of bias from T(1) and noise. *Magn Reson Med*. 2007; 58:354–364. [PubMed: 17654578]
13. Bydder M, Yokoo T, Hamilton G, Middleton MS, Chavez AD, Schwimmer JB, Lavine JE, Sirlin CB. Relaxation effects in the quantification of fat using gradient echo imaging. *Magn Reson Imaging*. 2008; 26:347–359. [PubMed: 18093781]
14. Hernando D, Liang ZP, Kellman P. Chemical shift-based water/fat separation: a comparison of signal models. *Magn Reson Med*. 2010; 64:811–822. [PubMed: 20593375]
15. Yu H, McKenzie CA, Shimakawa A, Vu AT, Brau AC, Beatty PJ, Pineda AR, Brittain JH, Reeder SB. Multiecho reconstruction for simultaneous water-fat decomposition and T2* estimation. *J Magn Reson Imaging*. 2007; 26:1153–1161. [PubMed: 17896369]
16. Yu H, Shimakawa A, McKenzie CA, Brodsky E, Brittain JH, Reeder SB. Multiecho water-fat separation and simultaneous R2* estimation with multifrequency fat spectrum modeling. *Magn Reson Med*. 2008; 60:1122–1134. [PubMed: 18956464]
17. Vasanawala SS, Yu H, Shimakawa A, Jeng M, Brittain JH. Estimation of liver T*2 in transfusion-related iron overload in patients with weighted least squares T*2 IDEAL. *Magn Reson Med*. 2012; 67:183–190. [PubMed: 21574184]
18. Hernando D, Kramer HJ, Reeder SB. Multipeak fat-corrected complex R2* relaxometry: theory, optimization, and clinical validation. *Magn Reson Med*. 2013
19. Zhong, X.; Nickel, MD.; Kannengiesser, SAR.; Dale, BM.; Kiefer, B.; Bashir, M. Fat and iron quantification using a multi-step adaptive fitting approach with multi-echo GRE imaging. Proceedings of the 21st Annual Meeting of ISMRM; Salt Lake City, Utah. 2013. p. 401
20. Yu H, Shimakawa A, Hines CD, McKenzie CA, Hamilton G, Sirlin CB, Brittain JH, Reeder SB. Combination of complex-based and magnitude-based multiecho water-fat separation for accurate quantification of fat-fraction. *Magn Reson Med*. 2011; 66:199–206. [PubMed: 21695724]
21. Hernando D, Hines CD, Yu H, Reeder SB. Addressing phase errors in fat-water imaging using a mixed magnitude/complex fitting method. *Magn Reson Med*. 2012; 67:638–644. [PubMed: 21713978]
22. Reeder SB, Robson PM, Yu H, Shimakawa A, Hines CD, McKenzie CA, Brittain JH. Quantification of hepatic steatosis with MRI: the effects of accurate fat spectral modeling. *J Magn Reson Imaging*. 2009; 29:1332–1339. [PubMed: 19472390]
23. Hansen KH, Schroeder ME, Hamilton G, Sirlin CB, Bydder M. Robustness of fat quantification using chemical shift imaging. *Magn Reson Imaging*. 2012; 30:151–157. [PubMed: 22055856]
24. Hernando D, Kuhn JP, Mensel B, Volzke H, Puls R, Hosten N, Reeder SB. R2* estimation using “in-phase” echoes in the presence of fat: the effects of complex spectrum of fat. *J Magn Reson Imaging*. 2013; 37:717–726. [PubMed: 23055408]
25. Kuhn JP, Hernando D, Munoz Del Rio A, Evert M, Kannengiesser S, Volzke H, Mensel B, Puls R, Hosten N, Reeder SB. Effect of multipeak spectral modeling of fat for liver iron and fat quantification: correlation of biopsy with MR imaging results. *Radiology*. 2012; 265:133–142. [PubMed: 22923718]
26. Kuroda K, Oshio K, Chung AH, Hynynen K, Jolesz FA. Temperature mapping using the water proton chemical shift: a chemical shift selective phase mapping method. *Magn Reson Med*. 1997; 38:845–851. [PubMed: 9358461]

27. Peters RD, Hinks RS, Henkelman RM. Ex vivo tissue-type independence in proton-resonance frequency shift MR thermometry. *Magn Reson Med*. 1998; 40:454–459. [PubMed: 9727949]
28. Quesson B, de Zwart JA, Moonen CT. Magnetic resonance temperature imaging for guidance of thermotherapy. *J Magn Reson Imaging*. 2000; 12:525–533. [PubMed: 11042633]
29. Kuroda K, Mulkern RV, Oshio K, Panych LP, Nakai T, Moriya T, Okuda S, Hynynen K, Jolesz FA. Temperature mapping using the water proton chemical shift: self-referenced method with echo-planar spectroscopic imaging. *Magn Reson Med*. 2000; 43:220–225. [PubMed: 10680685]
30. Rieke V, Butts Pauly K. MR thermometry. *J Magn Reson Imaging*. 2008; 27:376–390. [PubMed: 18219673]
31. Rieke V, Butts Pauly K. Echo combination to reduce proton resonance frequency (PRF) thermometry errors from fat. *J Magn Reson Imaging*. 2008; 27:673–677. [PubMed: 18064715]
32. Sprinkhuizen SM, Konings MK, van der Bom MJ, Viergever MA, Bakker CJ, Bartels LW. Temperature-induced tissue susceptibility changes lead to significant temperature errors in PRFS-based MR thermometry during thermal interventions. *Magn Reson Med*. 2010; 64:1360–1372. [PubMed: 20648685]
33. Grissom WA, Kerr AB, Holbrook AB, Pauly JM, Butts-Pauly K. Maximum linear-phase spectral-spatial radiofrequency pulses for fat-suppressed proton resonance frequency-shift MR Thermometry. *Magn Reson Med*. 2009; 62:1242–1250. [PubMed: 19780177]
34. Shmatukha AV, Harvey PR, Bakker CJ. Correction of proton resonance frequency shift temperature maps for magnetic field disturbances using fat signal. *J Magn Reson Imaging*. 2007; 25:579–587. [PubMed: 17335067]
35. Soher BJ, Wyatt C, Reeder SB, MacFall JR. Noninvasive temperature mapping with MRI using chemical shift water-fat separation. *Magn Reson Med*. 2010; 63:1238–1246. [PubMed: 20432295]
36. Wyatt C, Soher BJ, Arunachalam K, MacFall J. Comprehensive analysis of the Cramer-Rao bounds for magnetic resonance temperature change measurement in fat-water voxels using multi-echo imaging. *MAGMA*. 2012; 25:49–61. [PubMed: 21442434]
37. Hindman JC. Proton resonance shift of water in the gas and liquid states. *J Chem Phys*. 1966; 44:4582–4592.
38. Kuroda K, Suzuki Y, Ishihara Y, Okamoto K, Suzuki Y. Temperature mapping using water proton chemical shift obtained with 3D-MRSI: feasibility in vivo. *Magn Reson Med*. 1996; 35:20–29. [PubMed: 8771019]
39. Hamilton G, Yokoo T, Bydder M, Cruite I, Schroeder ME, Sirlin CB, Middleton MS. In vivo characterization of the liver fat (1)H MR spectrum. *NMR Biomed*. 2011; 24:784–790. [PubMed: 21834002]
40. Hines CD, Yu H, Shimakawa A, McKenzie CA, Brittain JH, Reeder SB. T1 independent, T2* corrected MRI with accurate spectral modeling for quantification of fat: validation in a fat-water-SPIO phantom. *J Magn Reson Imaging*. 2009; 30:1215–1222. [PubMed: 19856457]
41. Bydder M, Girard O, Hamilton G. Mapping the double bonds in triglycerides. *Magn Reson Imaging*. 2011; 29:1041–1046. [PubMed: 21868182]
42. Hu HH, Bornert P, Hernando D, Kellman P, Ma J, Reeder S, Sirlin C. ISMRM workshop on fat-water separation: insights, applications and progress in MRI. *Magn Reson Med*. 2012; 68:378–388. [PubMed: 22693111]
43. Imber CJ, St Peter SD, Handa A, Friend PJ. Hepatic steatosis and its relationship to transplantation. *Liver Transpl*. 2002; 8:415–423. [PubMed: 12004340]
44. Hamilton G, Middleton MS, Bydder M, Yokoo T, Schwimmer JB, Kono Y, Patton HM, Lavine JE, Sirlin CB. Effect of PRESS and STEAM sequences on magnetic resonance spectroscopic liver fat quantification. *J Magn Reson Imaging*. 2009; 30:145–152. [PubMed: 19557733]
45. Vanhamme L, van den Boogaart A, Van Huffel S. Improved method for accurate and efficient quantification of MRS data with use of prior knowledge. *J Magn Reson*. 1997; 129:35–43. [PubMed: 9405214]
46. Naressi A, Couturier C, Devos JM, Janssen M, Mangeat C, de Beer R, Graveron-Demilly D. Java-based graphical user interface for the MRUI quantitation package. *MAGMA*. 2001; 12:141–152. [PubMed: 11390270]

47. Yu, H.; Shimakawa, A.; Hernando, D.; Hines, CDG.; McKenzie, CA.; Reeder, SB.; Brittain, JH. Noise performance of magnitude-based water-fat separation is sensitive to the echo times. Proceedings of the 19th Annual Meeting of ISMRM; Montreal, Canada. 2011. p. 2715

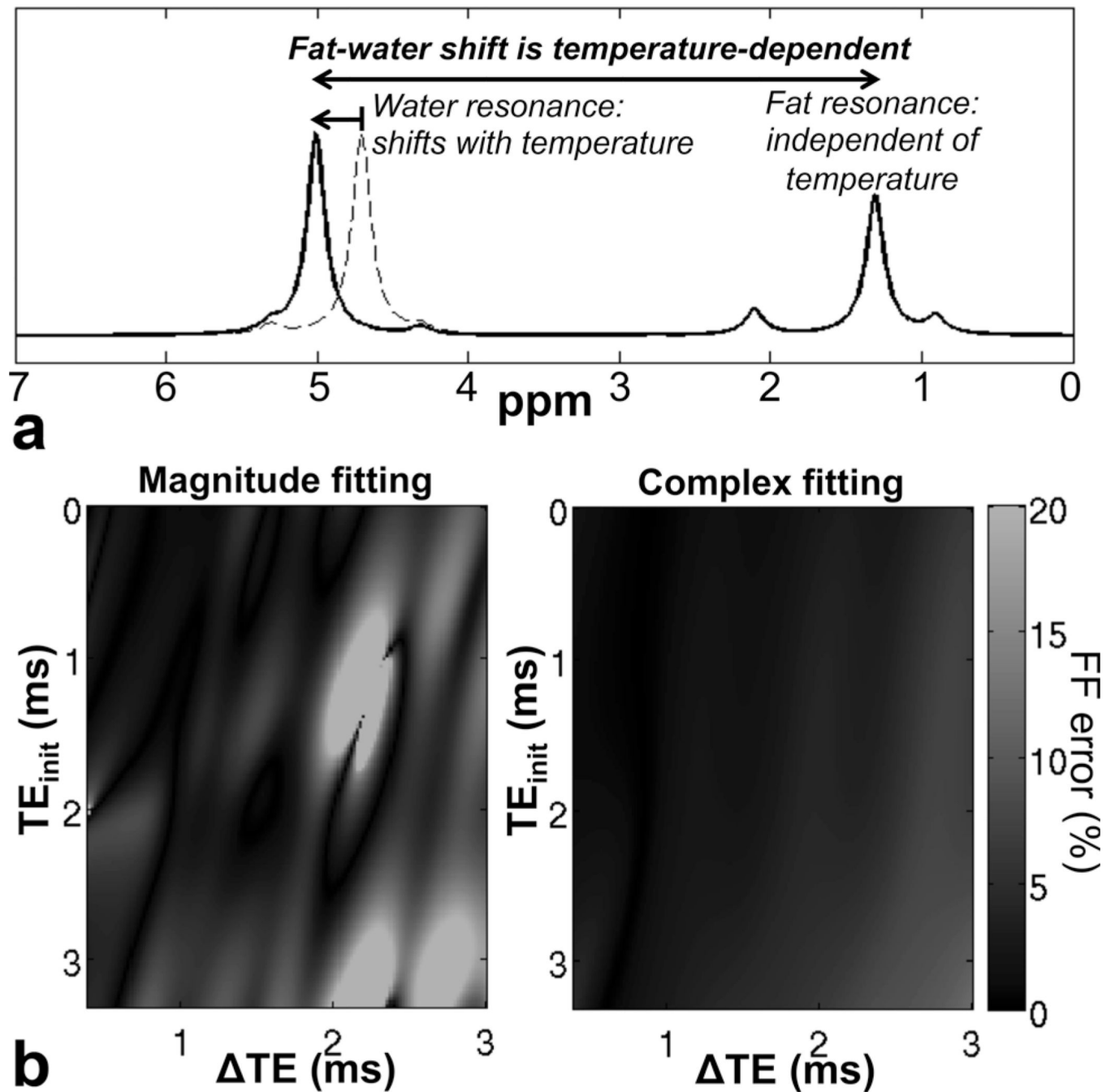


FIG. 1. Fat-water frequency shift is dependent on temperature, and can lead to errors in chemical shift-encoded fat quantification techniques. **a:** Schematic representation of temperature effects on fat-water signals, ignoring volume susceptibility effects, which affect both water and fat signals. Because of the temperature dependence of the water resonance due to electronic shielding of water protons, the fat-water shift is also temperature-dependent. **b:** Simulation plots show absolute FF estimation error as a function of TE combination when using a standard (temperature-uncorrected) signal model for fat quantification. Complex

fitting fat–water reconstructions result in moderate errors over a wide range of TE combinations. Magnitude fitting fat–water reconstructions result in large errors for certain TE combinations, especially $TE_{\text{init}} \approx 1.3$ ms, $TE \approx 2.2$ ms at 1.5T. The error (absolute %) of the fat-fraction related to temperature depends strongly on the type of reconstruction and on the choice of TE combination.

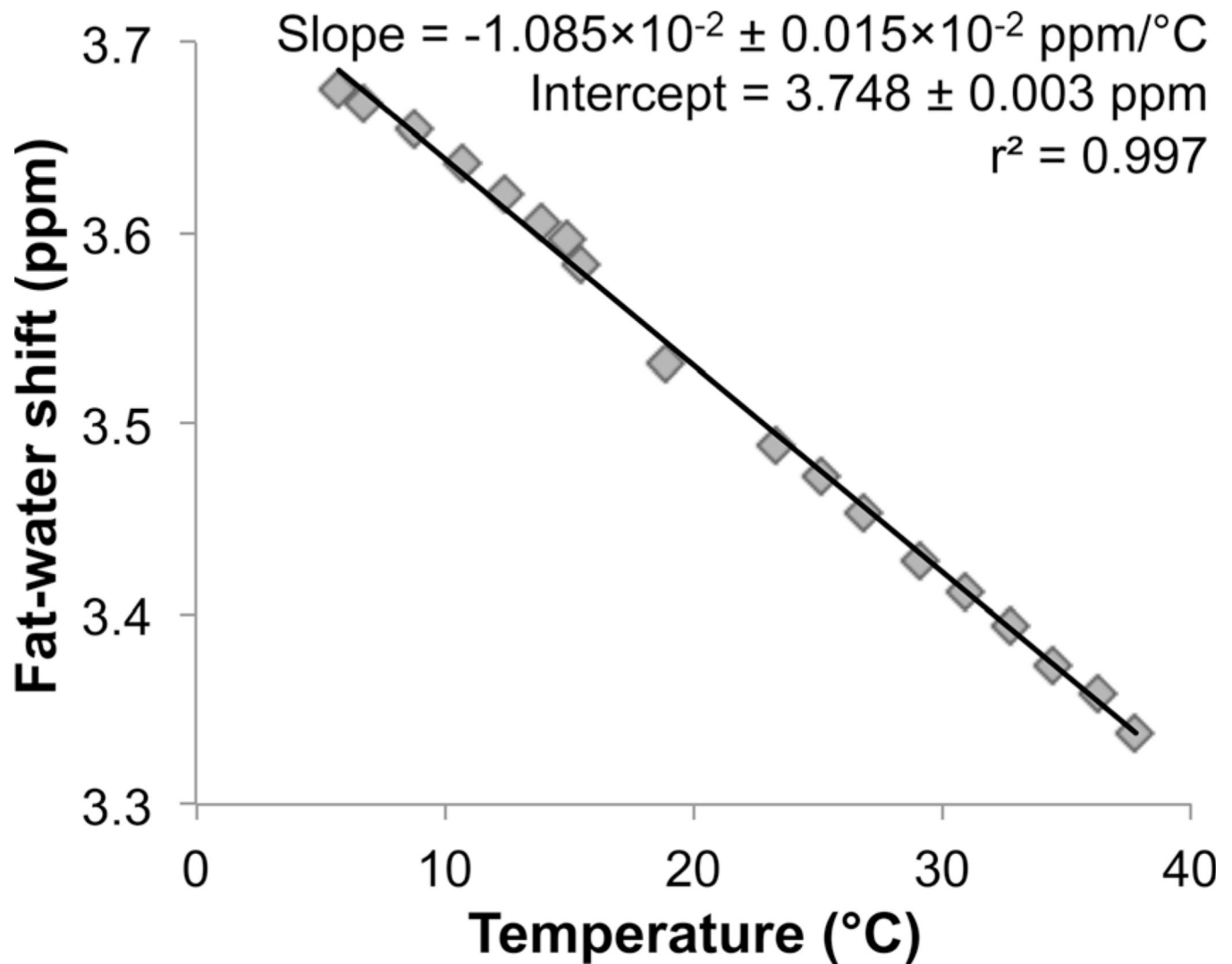


FIG. 2.

Fat–water frequency shift depends linearly on temperature over the range 0–40°C, as shown by the phantom experiments. The fat–water frequency shift varies with temperature, due to electron shielding effects on the water protons. In this phantom study, the fat–water shift as a function of temperature was determined from MR spectroscopy on a vial with FF = 50%. The slope from linear regression analysis was estimated to be $(-1.085 \pm 0.015) \times 10^{-2}$ ppm/°C, in good agreement with the literature (27).

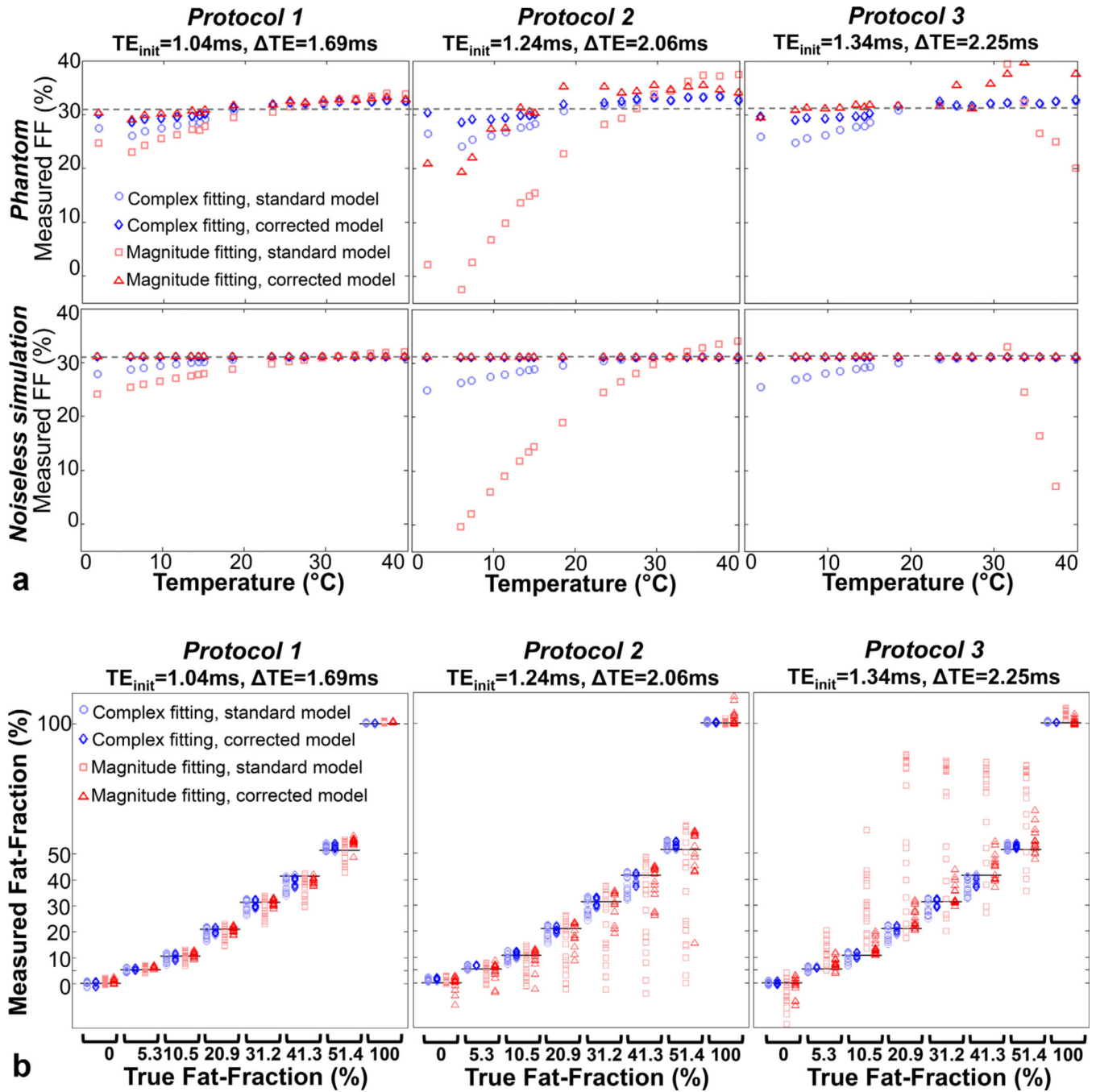


FIG. 3.

Phantom results demonstrate the sensitivity of fat quantification to temperature. **a:** Explicit temperature dependence (for true FF = 31.2%) shows increasing errors for larger temperature offsets relative to body temperature, in good agreement with simulations. **b:** For all phantom vials except FF = 0% and FF = 100%, standard magnitude fitting results in the largest variability in FF estimates over all temperatures. Temperature-corrected complex fitting generally results in the lowest variability. Complex fitting results in generally smaller errors than magnitude fitting, both in noiseless simulations and in phantoms. Remaining

errors in temperature-corrected reconstructions are possibly due to inaccuracies in the spectral fat–water model, or residual T1 bias effects. Note that T1 relaxation times are temperature-dependent, although this confounding factor is largely avoided in our techniques through the use of small flip angle acquisitions.

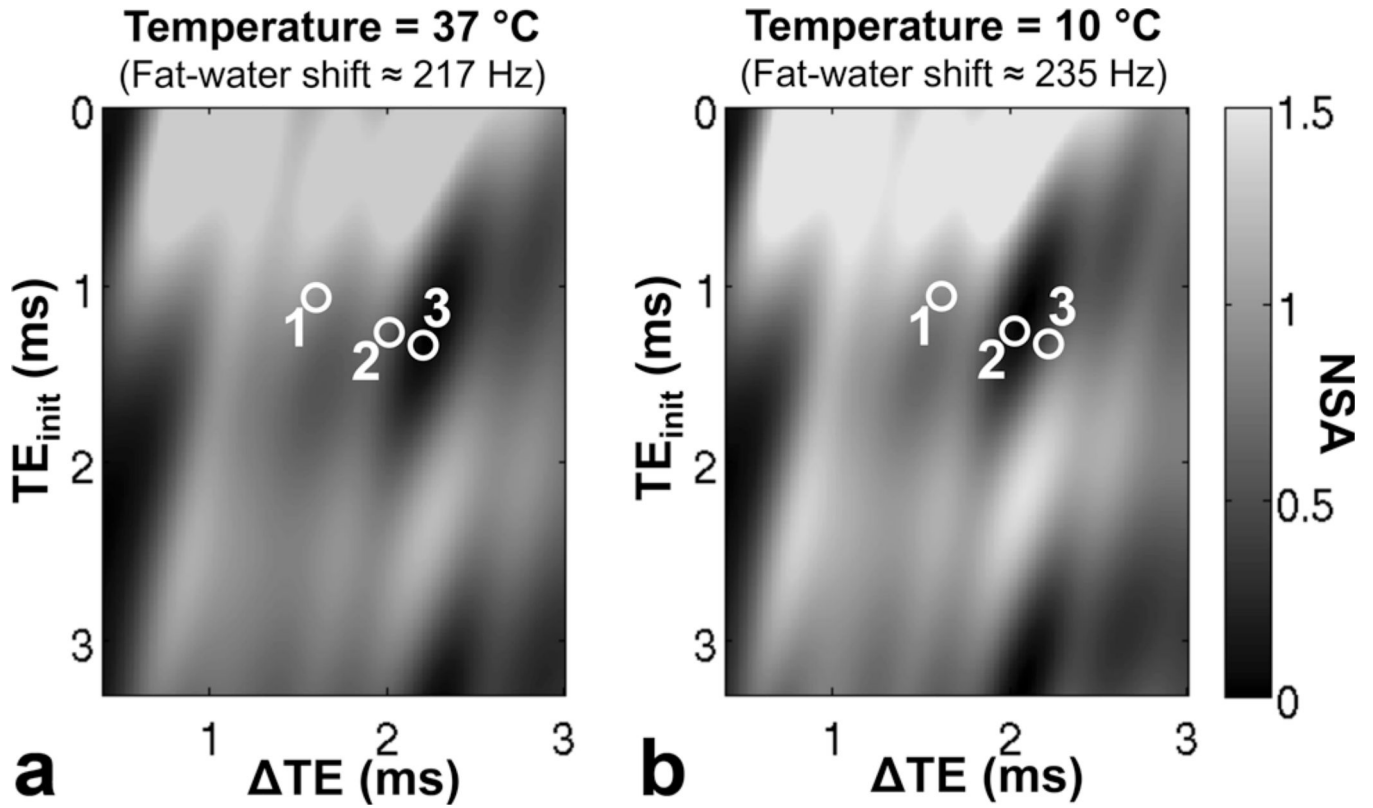


FIG. 4.

The noise performance of temperature-corrected magnitude fitting depends on the temperature and echo combination. The plots show the effective number of signal averages (NSA) for fat estimation using magnitude fitting as a function of TE combination: (a) at body temperature (37°C) as well as (b) at 10°C. Note that protocol 2 results in moderate noise performance for magnitude fitting at 37°C (217 Hz shift between water and the main methylene fat peak at 1.5T), but poor noise performance at 10°C (235 Hz shift). In contrast, protocol 3 actually demonstrated improved magnitude-fitting SNR performance at low temperatures. Note that noise performance is determined predominantly by the reconstruction model, rather than the underlying signal itself. Model mismatches such as those caused by temperature effects result in biased rather than noisy reconstructions.

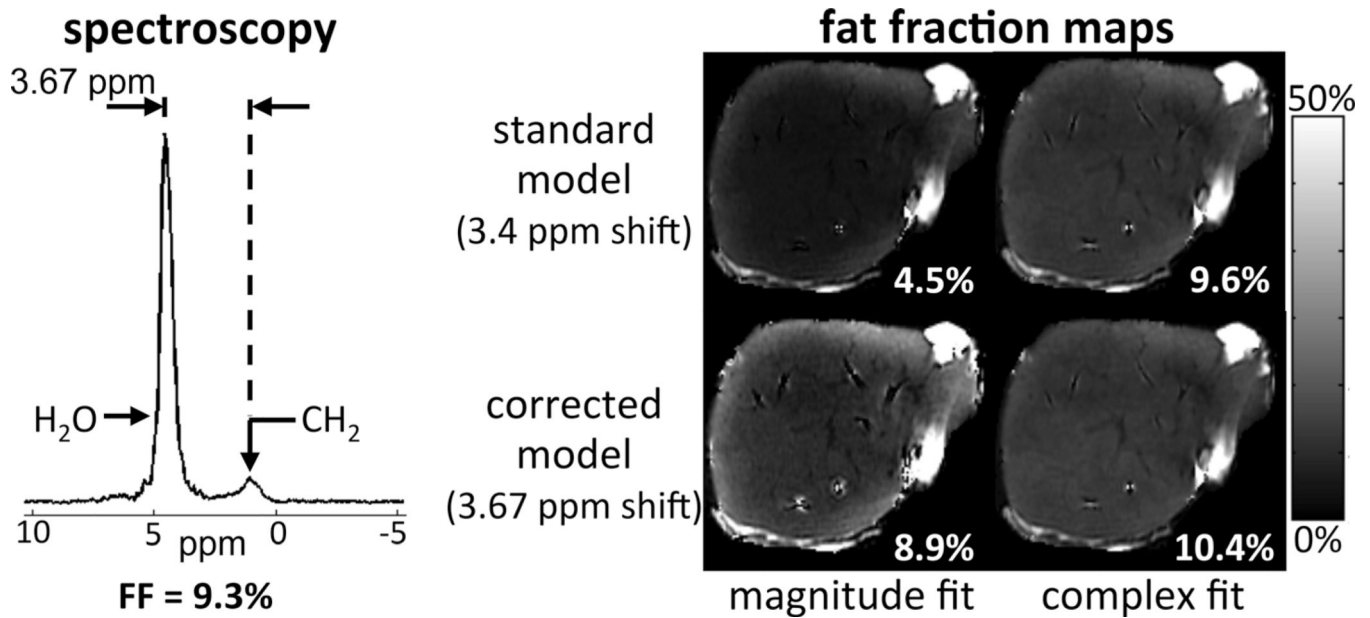


FIG. 5. Spectroscopy and chemical shift-encoded imaging results from an explanted liver. Fat quantification results are in good qualitative agreement with phantom and simulation results. Using spectroscopy as the reference standard, complex fitting and/or temperature-corrected modeling resulted in improved accuracy in fat-quantification.